NUCLEAR SCIENCE AND TECHNIQUES **26**, 060502 (2015)

A facile method for studying interaction of rhodamine B and bovine serum albumin: Towards physical-binding mediated fluorescence labeling of proteins*

MA Yu-Xing (马宇星), ZHONG Rui-Bo (钟睿博), GUO Jun (郭俊), LIU Yu-Shuang (刘雨双), YUAN Ming (袁鸣), BAI Zhi-Jun (白志军), LIU Tao-Tao (刘涛涛), ZHAO Xin-Min (赵欣敏), and ZHANG Feng (张峰)†

Agricultural Nanocenter, School of Life Sciences, Inner Mongolia Agricultural University, Hohhot 010018, China

(Received June 8, 2015; accepted in revised form August 2, 2015; published online December 20, 2015)

Strategies for labeling proteins with fluorophores are always important for biotechnology. Here we take a model protein (bovine serum albumin) and a typical fluorophore (rhodamine B) to demonstrate a direct labeling method just by physical adsorption. In combination with size exclusion chromatography and the Scartchard equation, we have developed a facile analysis method for calculating the binding constant and binding sites. The molecular docking method has been used to study the binding site in amino acid level.

Keywords: Bovine serum albumin, Rhodamine B, Binding sites, Scatchard equation, Size exclusion chromatography

DOI: 10.13538/j.1001-8042/nst.26.060502

I. INTRODUCTION

Fluorescence labeling of proteins, especially antibodies, has been widely used in current biotechnology applications. Generally, there are two requirements for a successful bio-labeling: 1) both original functionality of bio-molecules and original fluorescence property of the markers must be kept intact after labeling; and 2) the labeling should be robust enough in subsequent applications. Protein labeling kits are commercially available from Invitrogen, Sigma-Aldrich, etc. The labeling technologies can be classified as chemical conjugation and physical binding. The former includes carbodiimide mediated crosslinking of carboxylic groups and primary amino groups, and the azide and alkyne mediated click chemistry, while the latter includes bio-melocular pair-mediated labeling using DNA, biotin-avidin, aptamer-target, protein A/G-antibody, ligand-receptor, and antigen-antibody. Although fluorescent nanoparticles like semiconductor quantum dots [1–4], graphene quantum dots [5–7], nanodiamonds [8–10], fluorescence carbon dots [11, 12] have attracted increasing interest for both labeling/imaging and sensing due to their perfect photostability, organic dyes are still playing main labeling role with the concern of toxicities and size limitations.

Rhodamine B (RB), as a dye or a dye laser gain medium [13, 14], is often used as a tracer dye within water to determine the rate and direction of flow and transport. Due to its good solubility in water (~ 15 g/L), high quantum yield (about 94%), and the fact that its fluorescence can be easily and inexpensively detected by a fluorometer, RB has been extensively used as a biomaker in biotechnological labeling and imaging in fluorescence microscopy, flow cytometry, fluorescence correlation spectroscopy (FCS) and enzyme-linked immunosorbent assay (ELISA).

Bovine serum albumin (BSA), also known as "fraction V", which refers to albumin being the fifth fraction of the original Edwin Cohn purification methodology that made use of differential solubility characteristics of plasma proteins [15], is a serum albumin protein derived from cows. And due to its stability, low-cost and clear structural information, BSA has been used as a model protein for many research aims, for example it can be used as a protein concentration standard in lab experiments, and its amphiphilic property has also made itself as a good carrier for both natural and artificial drugs like vitamins and paclitaxel. The mature BSA protein contains 583 amino acids (Mw 66 463 Da, 66.5 kDa), which is a product from twice enzymatic cleavages from a 607-amino-acid full-length BSA precursor protein [16].

In this paper, we take the conventional fluorophore RB and the model protein BSA as objects for an interaction study towards a direct labeling method. With an idea to develop a new facile analysis approach based on the size exclusion chromatography (SEC), the association constant/binding affinity (K_a) and the maximum binding sites of RB to BSA have been determined by employing the well-known Scartchard equation, and the detailed interaction information is further studied by using molecular docking.

II. EXPERIMENTAL SECTION

A. Materials

BSA (lyophilized powder $>98\%$), RB ($>99\%$) and all other chemical regents were purchased from Sigma-Aldrich Corporation. Deionized water (18.2 MΩ cm) from a Milli-Q system (Millipore, Bedford, MA) was used for all experiments. BSA was dissolved in Milli-Q water for a stock solution with a concentration of 600 μM. RB was dissolved in Milli-Q water with a stock concentration of 600 μM.

* Supported by the National Natural Science Foundation of China (Nos. 21171086 and 81160213), Inner Mongolia Autonomous Region science and Technology Department (No. 211-202077), Inner Mongolia Grassland Talent (No. 108-108038), Natural Science Foundation of Inner Mongolia Autonomous Region of China (No. 2013MS1121) and Inner Mongolia Agricultural University (Nos. 109-108040, 211-109003 and 211-206038)

† Corresponding author, fengzhang1978@hotmail.com

B. Spectroscopic measurements

UV-vis absorption spectra were recorded on a U-2900 UV-vis spectrometer (Hitachi).

C. SEC assays

The SEC assays were performed on a sephacryl S-300 column equipped with a high performance liquid chromatography (HPLC) system (Hitachi L2000 or Agilent 1260) with a flow phase of SB9 (sodium borate 50 mM, pH = 9) buffer and the flow rate of 1 mL/min. The spectra were monitored at 280 nm for UV detector and excitation (Ex): 555 nm / emission (Em): 575 nm for the fluorescence detector. For the fluorometric titration experiment, 995 μL solutions containing different RB/BSA ratios of 64/1, 32/1, 16/1, 8/1 and 4/1 with a fixed final BSA concentration of 2.29 nM was prepared and incubated at 298 K for 2 h.

D. Molecular docking

The three-dimensional (3D) structure of the BSA (PDB ID: 4JK4) was downloaded from Protein Data Bank (http://www.rcsb.org/pdb/home/home.do). The Auto Dock Tools 1.5.6 package (http://mgltools.scripps.edu) was employed to generate the docking input files. The search grid of BSA was identified as center x: 97.127, center y: 24.933, and center z: 20.919 with dimensions size x: 15, size y: 15, and size z: 15. For Vina docking, the default parameters were used if it was not mentioned. The best-scoring pose as judged by the Vina docking score is chosen and visually analyzed using PyMOL software (http://www.pymol.org/).

III. RESULTS AND DISCUSSION

A. Binding constant and binding sites

A number of methods can be used to calculate/measure the binding constant and binding sites. Some authors like using fluorescence quenching [17–19] to study interactions between proteins and other molecules. This method is facile and easily accessible, but it is limited when the molecules are not quenchers to proteins' fluorescence. Other popular methods include quartz crystal microbalance (QCM)-based [20], and surface plasmon resonance (SPR)-based [21] techniques, but they cost quite a lot by consuming specific chips. The raw data obtained with these methods normally need further processing in combination with some classical equations, like Stern-Volmer equation, Scatchard equation and Hill equation, to get the binding constants, sites and even cooperativity.

SEC is a powerful tool for both analysis and separation. Because proteins are several times larger than the labeling fluorophores which are normally less than 1 nm, so we can readily separate the bound fluorophores and free ones, which is exactly the data required by the Scatchard equation,

$$\nu/C_{\mathrm{f(RB)}} = (n-\nu)K_{\mathrm{a}}, \tag{1}$$

where C_{f} is concentration of the free ligand, which in our case is the unbound RB's concentration; n is the number of binding sites per protein molecule; K_{a} is the association/binding constant/affinity of RB for BSA; and ν is the real bound ratio defined as,

$$\nu = (C_{\mathrm{t(RB)}} - C_{\mathrm{f(RB)}})/C_{\mathrm{t(BSA)}}, \tag{2}$$

where $C_{\mathrm{t(RB)}}$ is concentration of total RB which is known before the binding assay; $C_{\mathrm{f(RB)}}$ is the free or unbound RB's concentration which can be obtained by SEC measurement; and $C_{\mathrm{t(BSA)}}$ is concentration of total BSA for the binding assay, which is known and constant in the current assay.

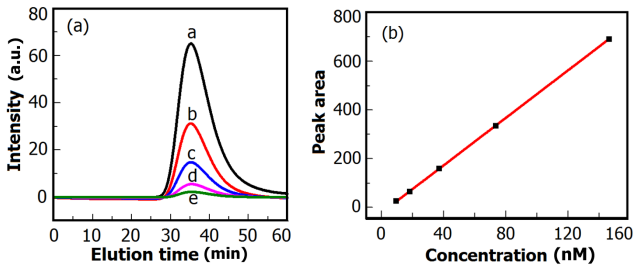

Fig. 1. (Color online) Concentration calibration of RB obtained by SEC. (a) Fluorescence signals obtained by SEC at RB concentrations of (from a to e) 146.4 nM, 73.24 nM, 36.62 nM, 18.31 nM and 9.15 nM. (b) The calibration curve of free RB's concentration ($C_{\mathrm{f(RB)}}$) based on the SEC by plotting the elution peak area against the concentration.

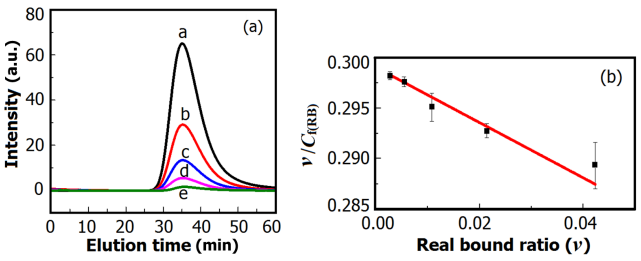

Fig. 2. (Color online) The binding assay studied by SEC and Scatchard equation. (a) Fluorescence signals derived from the SEC analysis at RB/BSA molar ratios of 64/1, 32/1, 16/1, 8/1 and 4/1 (from a to e). The peaks reflect the free RB's concentration ($C_{\mathrm{f(RB)}}$), and the conjugate's concentration was too low compared with the free RB's eluted out at 10 min. (b) The Scatchard plot and linear fit.

We took RB and BSA for an example to justify the use of SEC in combination with Scatchard equation to calculate the binding constant and sites between molecules and proteins. To be more precisely, we made a pure dye's SEC to get the SEC-based calibration curve of concentration (Fig. 1) by plotting the integrated elution peaks against the concentrations. From Fig. 2, it can be seen that, with the molar ratios of

RB/BSA in Section II C, the RB's fluorescence intensity decreases linearly with increasing BSA/RB ratios at a fixed RB molar concentration. The binding constant and binding sites were calculated at $2.2 \times 10^5\,\mathrm{M}^{-1}$ and 1.3, respectively. Cai *et al*. reported that the binding constant and binding sites were $4.8 \times 10^4\,\mathrm{M}^{-1}$ and 1.2, respectively. However, their further analysis by time-resolved fluorescence indicated at least two binding sites existed [22]. The real binding sites can be highly resolved by crystallographic studies of the complexes of proteins and molecules, for example Sekula B. and colleagues found there are four binding sites of 3,5-diiodosalicylic acid to BSA [23]. The binding affinity obtained by the current method seems much higher than Ref. [22]. Thus, we believe that different buffers and sensitivities of the instruments might be the culprit, and that the fluorescence quenching method can produce huge deviations for the binding affinity evaluation [24]. So, it would be helpful to compare different methods in the same conditions.

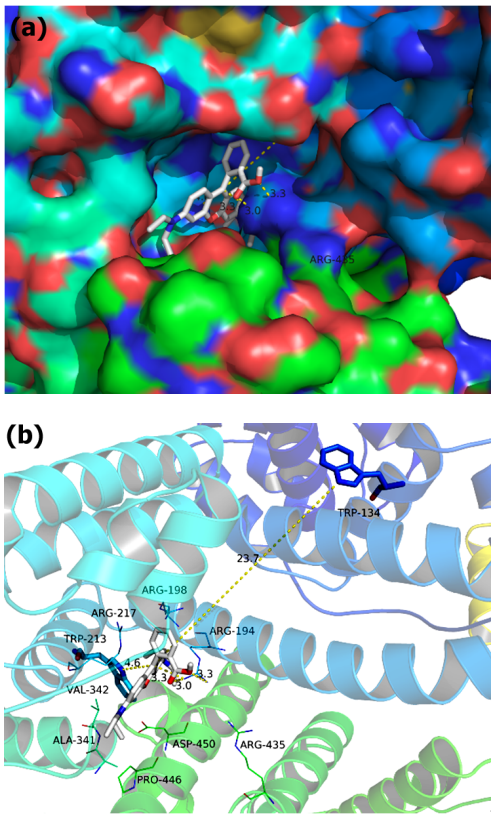

Fig. 3. (Color online) Molecular docking of RB and BSA. (a) The RB is docked into binding pocket of the BSA's surfaced structure. (b) Detailed analysis of main binding affinity between BSA's amino acid residues and RB's chemical groups. The distances are in Å (0.1 nm).

It is not difficult to find the intermolecular interaction studies by searching the scientific publication bank/library, but it may be difficult to figure out how those scientists get necessary values for the Scatchard plot. By using SEC assisted with an HPLC system, one can clearly learn how to do this plot step-by-step. With the well-known reputation of the repeatability of a commercial HPLC system such as the Agilent used in this paper, one can directly calculate both binding constant and binding sites just by simply preparing the mixture solution. In addition, the concentration calibration curve of free dye alone obtained by the same configuration constants of HPLC system such as the column, flow rates and loading volumes, is necessary in that it minimizes the measurement error.

B. Molecular docking of RB and BSA

To study the binding mode of RB to BSA, molecular docking was performed by using the Auto dock. As shown in Fig. 3, the RB molecule is docked into the binding pocket of the BSA. One of diethylamino group of RB fits into bottom of the binding pocket of BSA, surrounded by the residues Trp^{213}, Arg^{194} and Arg^{198}, while the other diethylamino group located at the entrance of the pocket, interacted with the hydrophobic residues Val^{342}, Ala^{341} and Pro^{446}. Importantly, the carboxyl group forms two key hydrogen bonds (2.0 and 3.3 Å) with the residue Arg^{194}, which is important for the affinity between RB and BSA.

In summary, the computational approach helps in better understanding of inhibitors binding to the protein active site, which provides valuable information for further study of interaction between RB and BSA. Limited by the docking software which does not support the multi-molecular docking, we didn't try more docking sites.

IV. CONCLUSION

Compared with different chemical labeling strategies, the direct labeling method with such a high binding affinity will hold great promise for future biotechnology. The facile method in combination with SEC and Scatchard equation has shown the feasibility to get the binding constant and sites of BSA-RB interaction, which might find more applications in other proteins and small molecules or any two substances with large size differences. We hope this study could also make a good example for demonstrating a well combination of experimental measurements and theoretical simulations.

[1] Li C Y, Li Q, Liu H T, *et al*. Hot topic and challenge of semiconductor quantum dots as fluorescence labels. Prog Biochem Biophys, 2010, **37**: 103–110. DOI: 10.3724/SP.J.1206.2009.00342

[2] Gao X, Cui Y, Levenson R M, *et al*. *In vivo* cancer targeting and imaging with semiconductor quantum dots. Nat Biotecnol,

2004, **22** : 969–976. DOI: 10.1038/nbt994
[3] Jin Y and Gao X. Plasmonic fluorescent quantum dots. Nat Biotecnol, 2009, **4** : 571–576. DOI: 10.1038/NNANO.2009.193
[4] Zhang F, Lees E, Amin F, *et al*. Polymer-coated nanoparticles: A universal tool for biolabelling experiments. Small, 2011, **7** : 3113–3127. DOI: 10.1002/smll.201100608
[5] Tang L, Ji R, Cao X, *et al*. Deep ultraviolet photoluminescence of water-soluble self-passivated graphene quantum dots. Acs Nano, 2012, **6**: 5102–5110. DOI: 10.1021/nn300760g
[6] Wang L, Zhu S J, Wang H Y, *et al*. Common origin of green luminescence in carbon nanodots and graphene quantum dots. Acs Nano, 2014, **8**: 2541–2547. DOI: 10.1021/nn500368m
[7] Eda G, Lin Y Y, Mattevi C, *et al*. Blue photoluminescence from chemically derived graphene oxide. Adv Mater, 2010, **22**: 505–509. DOI: 10.1002/adma.200901996
[8] Huang H J, Pierstorff E, Osawa E, *et al*. Protein-mediated assembly of nanodiamond hydrogels into a biocompatible and biofunctional multilayer nanofilm. Acs Nano, 2008, **2**: 203–212. DOI: 10.1021/nn7000867
[9] Liu J H, Yang S T, Chen X X, *et al*. Fluorescent carbon dots and nanodiamonds for biological imaging: preparation, application, pharmacokinetics and toxicity. Curr Drug Metab, 2012, **13**: 1046–1056. DOI: 10.2174/138920012802850083
[10] Fu C C, Lee H Y, Chen K, *et al*. Characterization and application of single fluorescent nanodiamonds as cellular biomarkers. P Natl A Sci USA, 2007, **104**: 727–732. DOI: 10.1073/pnas.0605409104
[11] Zheng M, Liu S, Li J, *et al*. Integrating oxaliplatin with highly luminescent carbon dots: An unprecedented theranostic agent for personalized medicine. Adv Mater, 2014, **26**: 3554–3560. DOI: 10.1002/adma.201306192
[12] Anilkumar P, Cao L, Yu J J, *et al*. Crosslinked carbon dots as ultra-bright fluorescence probes. Small, 2013, **9**: 545–551. DOI: 10.1002/smll.201202000
[13] Schäfer F P and Drexhage K H. Dye lasers. New York (USA): Springer-Verlag, 1990.
[14] Duarte F J, Hillman L W, Liao P F, *et al*. Dye laser principles: with applications. Boston (USA): Academic Press, 1990.
[15] Tanaka K, Shigueoka E M, Sawatani E, *et al*. Purification of human albumin by the combination of the method of Cohn with liquid chromatography. Braz J Med Biol Res, 1998, **31**: 1383–1388. DOI:10.1590/S0100-879X1998001100003
[16] Peters Jr T. 3 - Serum albumin. In: Putnam F W, editor. The plasma proteins (Second Edition). Massachusetts (USA): Academic Press, 1975, 133–181.
[17] Yuan M, Zhong R, Yun X, *et al*. A fluorimetric study on the interaction between a Trp-containing beta-strand peptide and amphiphilic polymer-coated gold nanoparticles. Luminescence, 2015, online version. DOI:10.1002/bio.2920
[18] Liu Y S, Zhang P, Zhong R, *et al*. Fluorimetric study on the interaction between fluoresceinamine and bovine serum albumin. Nucl Sci Tech, 2015, **26**: 030505. 10.13538/j.1001-8042/nst.26.030505
[19] Zhong R B, Liu Y S, Zhang P, *et al*. Discrete nanoparticle-BSA conjugates manipulated by hydrophobic interaction. Acs Appl Mater Inter, 2014, **6**: 19465–19470. DOI: 10.1021/am506497s
[20] Ma H, He J, Zhu Z, *et al*. A quartz crystal microbalance-based molecular ruler for biopolymers. Chem Commun, 2010, **46**: 949–951. DOI: 10.1039/b919179h
[21] Jin Y D. Multifunctional compact hybrid Au nanoshells: A new generation of nanoplasmonic probes for biosensing, imaging, and controlled release. Accounts Chem Res, 2014, **47**: 138–148. DOI: 10.1021/ar400086e
[22] Cai H H, Zhong X, Yang P, *et al*. Probing site-selective binding of rhodamine B to bovine serum albumin. Colloid Surface A, 2010, **372**: 35–40. DOI:10.1016/j.colsurfa.2010.09.017
[23] Sekula B, Zielinski K and Bujacz A. Crystallographic studies of the complexes of bovine and equine serum albumin with 3,5-diiodosalicylic acid. Int J Biol Macromol, 2013. **60**: 316–324. DOI: 10.1016/j.ijbiomac.2013.06.004
[24] Boulos S P, Davis T A, Yang J A, *et al*. Nanoparticle-protein interactions: a thermodynamic and kinetic study of the adsorption of bovine serum albumin to gold nanoparticle surfaces. Langmuir, 2013, **29**: 14984–14996. DOI: 10.1021/la402920f